High-Resolution Solid-State H-2 NMR Spectroscopy of Polymorphs of Glycine

ARTICLE *in* THE JOURNAL OF PHYSICAL CHEMISTRY A · SEPTEMBER 2011

Impact Factor: 2.69 · DOI: 10.1021/jp207592u · Source: PubMed

THE JOURNAL OF PHYSICAL CHEMISTRY A

ARTICLE

pubs.acs.org/JPCA

High-Resolution Solid-State ^{2}H NMR Spectroscopy of Polymorphs of Glycine

Abil E. Aliev,*[,†] Sam E. Mann,[†] Aisha S. Rahman,[†] Paul F. McMillan,[†] Furio Corà,[†] Dinu Iuga,[‡] Colan E. Hughes,[§] and Kenneth D. M. Harris*[,§]

[†]Department of Chemistry, University College London, 20 Gordon Street, London WC1H 0AJ, United Kingdom

[‡]Department of Physics, University of Warwick, Coventry CV4 7AL, United Kingdom

[§]School of Chemistry, Cardiff University, Park Place, Cardiff CF10 3AT, Wales

ABSTRACT: High-resolution solid-state ^{2}H MAS NMR studies of the α and γ polymorphs of fully deuterated glycine (glycine-d_5) are reported. Analysis of spinning sideband patterns is used to determine the ^{2}H quadrupole interaction parameters, and is shown to yield good agreement with the corresponding parameters determined from single-crystal ^{2}H NMR measurements (the maximum deviation in quadrupole coupling constants determined from these two approaches is only 1%). From analysis of simulated ^{2}H MAS NMR sideband patterns as a function of reorientational jump frequency (κ) for the $-N^+D_3$ group in glycine-d_5, the experimentally observed differences in the ^{2}H MAS NMR spectrum for the $-N^+D_3$ deutrons in the α and γ polymorphs is attributed to differences in the rate of reorientation of the $-N^+D_3$ group. These simulations show severe broadening of the ^{2}H MAS NMR signal in the intermediate motion regime, suggesting that deuterons undergoing reorientational motions at rates in the range $\kappa \approx 10^4-10^6$ s^{-1} are likely to be undetectable in ^{2}H MAS NMR measurements for materials with natural isotopic abundances. The ^{1}H NMR chemical shifts for the α and γ polymorphs of glycine have been determined from the ^{2}H MAS NMR results, taking into account the known second-order shift. Further quantum mechanical calculations of ^{2}H quadrupole interaction parameters and ^{1}H chemical shifts reveal the structural dependence of these parameters in the two polymorphs and suggest that the existence of two short intermolecular C−H···O contacts for one of the H atoms of the $>CH_2$ group in the α polymorph have a significant influence on the ^{2}H quadrupole coupling and ^{1}H chemical shift for this site.

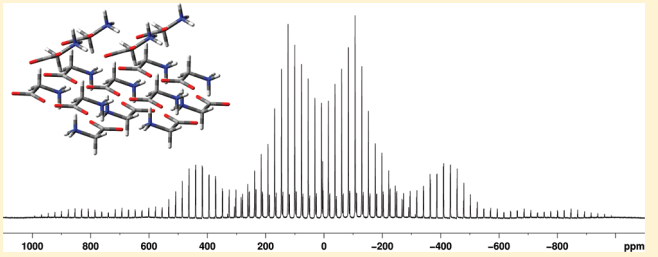

1. INTRODUCTION

It is well established from both solution-state and solid-state NMR data that ^{1}H chemical shifts are highly sensitive to local structural features, including molecular conformation, hydrogen bonding, and weak noncovalent interactions such as intermolecular C−H···O close contacts. As a consequence, ^{1}H NMR measurements have the potential to yield significant insights concerning subtle differences in the structural properties of polymorphs in the solid state. Unfortunately, however, the routine measurement of well-resolved ^{1}H NMR spectra for solids is complicated significantly by strong homonuclear ^{1}H···^{1}H dipole-dipole interactions. Nevertheless, it is important to recognize that ^{1}H and ^{2}H NMR chemical shifts are essentially the same (subject to small second-order shifts that can be readily determined),[1−4] and thus ^{1}H chemical shifts can be determined straightforwardly via high-resolution solid-state ^{2}H NMR measurements. The measurement of high-resolution ^{2}H NMR spectra for solids is substantially more straightforward than measurement of the corresponding ^{1}H NMR spectra, as ^{2}H NMR spectra can be recorded using standard heteronuclear ^{1}H decoupling and magic angle sample spinning (MAS).[3−8] The only significant drawback of solid-state ^{2}H NMR arises from the very low natural abundance of the ^{2}H isotope (∼0.0115%),[9] and the inherently low sensitivity of the technique dictates that isotopic labeling of materials for ^{2}H NMR studies of solids is usually necessary, although progress has also been made in recording solid-state ^{2}H NMR spectra for materials with natural isotopic abundance. Thus, we have shown recently that natural-abundance solid-state ^{2}H NMR spectroscopy can be applied successfully to study structural and dynamic properties of solids.[1]

An additional advantage of high-resolution solid-state ^{2}H NMR is that ^{2}H quadrupole interaction parameters (i.e., the quadrupole coupling constant χ and asymmetry parameter η) can be estimated from the same spectra used for chemical shift measurements. Thus, in principle, the intensity distribution of spinning sidebands in ^{2}H MAS NMR spectra provides a straightforward means for estimating the ^{2}H quadrupole interaction parameters, although more accurate ways of determining these parameters (e.g., from ^{2}H NMR studies of single-crystal samples or nonspinning polycrystalline powders) are clearly desirable in many cases. ^{2}H quadrupole coupling constants for organic materials are typically of the order of ∼200 kHz, which is

Received: August 8, 2011
Revised: September 21, 2011
Published: September 22, 2011

of a similar order of magnitude to the frequencies of various reorientational motions that can occur in organic solids in an appropriate temperature regime. Thus, the ^{2}H quadrupole interaction is sensitive to motional averaging effects due to dynamic processes of this type, and measurements of the ^{2}H quadrupole interaction parameters can yield detailed information on solid-state dynamics.[10]

In this paper, we explore the opportunities provided by high-resolution solid-state ^{2}H NMR, employing both experimental and computational techniques in studies of the α and γ polymorphs of fully deuterated glycine (glycine-d_5). From experimental ^{2}H MAS NMR spectra, we assess the opportunity to exploit the analysis of spinning sideband intensity distributions for accurate determination of ^{2}H quadrupole interaction parameters. We also employ numerical simulations to investigate the dependence of the intensity and shape of the spinning sideband pattern, and the line width of the isotropic ^{2}H NMR signal, on the time scale of reorientational motions (specifically for the $-N^+D_3$ group in glycine-d_5). Finally, quantum mechanical (QM) chemical shift calculations are used to analyze the ^{1}H chemical shifts measured from high-resolution ^{2}H NMR spectra, and their sensitivity to weak intermolecular interactions is assessed.

One of the primary objectives of this study is to prepare grounds for future high-resolution solid-state ^{2}H NMR measurements on materials with natural isotopic abundances. In spite of the low natural abundance of the ^{2}H isotope, the increasing availability of high-field NMR instruments (greater than 20 T) creates the prospect of carrying out natural-abundance ^{2}H NMR measurements on a routine basis, particularly for full structural and dynamics studies of polymorphism in organic solids (including pharmaceutical materials) as well as for fundamental studies of intermolecular and intramolecular interactions in the solid state.

2. BACKGROUND TO POLYMORPHISM IN GLYCINE

Glycine has been studied widely in polymorphism research[11−16] and has acquired the status of a prototypical system in this regard. Under ambient conditions, three polymorphs of glycine (denoted α, β and γ) are known,[11−13] and in each polymorph, the molecule exists in the zwitterionic form ($H_3N^+CH_2CO_2^-$). The γ polymorph is thermodynamically stable under ambient conditions, with the following order of stability: $\gamma > \alpha > \beta$.[14] The consensus in the literature is that crystallization of glycine from aqueous solution at neutral pH leads to the metastable α polymorph, whereas the stable γ polymorph is obtained by crystallization from basic (pH > ∼8.9) or acidic (pH < ∼3.8) aqueous solutions. Several other strategies have been reported to induce the formation of the γ polymorph,[15] including addition of sodium salts to the crystallization solution, application of polarized laser radiation or a d.c. electric field, evaporation of microdroplets, or thin-film evaporation from a glass surface. As a result of the complexity of the crystallization behavior of glycine, it has also served as a model system for exploring fundamental aspects of crystallization processes.[16]

3. EXPERIMENTAL SECTION

Fully deuterated glycine (glycine-d_5; $D_3N^+CD_2COO^-$; 98.2 atom % D) was purchased from MSD Isotopes. From the ^{1}H MAS NMR spectrum recorded at MAS frequency 14 kHz, the ammonium-to-methylene ratio is 0.7:1. Given that ^{1}H and ^{2}H are not evenly distributed between the ammonium and methylene groups, we have estimated the individual percentages of deuteration in each group: ammonium, 98.8%; methylene, 97.4%. This sample was shown by powder X-ray diffraction to be a monophasic sample of the α polymorph. A sample of the γ polymorph of glycine-d_5 was prepared by crystallization from a solution containing 0.5 g of the above sample of glycine-d_5 and 0.325 g of sodium hydroxide-h_1 dissolved in 1.74 g of D_2O (the sodium hydroxide raises the pH of the solution to 9.6).[16d] The solution was left to evaporate, and crystals were harvested before complete evaporation of solvent had occurred. From the ^{1}H MAS NMR spectrum recorded at MAS frequency 14 kHz, the ammonium-to-methylene integration ratio is 7:1. When this ratio and that in the α polymorph of glycine-d_5 were used (see above), we have estimated the individual percentages of deuteration in each group: ammonium, 87.6%; methylene, 97.4%. The collected crystals were shown by powder X-ray diffraction to be a monophasic sample of the γ polymorph.

Solid-state ^{1}H and ^{2}H NMR spectra were recorded at ambient probe temperature at 850.22 and 130.51 MHz, respectively, on a Bruker AVANCE III 850 NMR spectrometer at the UK 850 MHz Solid-State NMR Facility at the University of Warwick. All samples were studied as polycrystalline powders in zirconia rotors (4 mm external diameter). High-resolution solid-state ^{2}H NMR spectra were recorded using a single-pulse sequence, with the sample subjected to MAS and with ^{1}H decoupling applied during acquisition using the SPINAL-64 sequence.[17] Typical operating conditions were: ^{2}H 90° pulse duration, 5 μs; recycle delay, 20−300 s; acquisition time, 100 ms. ^{2}H CPMAS NMR spectra were also recorded using ^{1}H → ^{2}H cross-polarization (CP contact time, τ_{CP} = 1 ms) together with MAS and ^{1}H decoupling using SPINAL-64. Data acquisition and processing were performed using standard Bruker TopSpin (version 2.1) software. Line widths were measured using the *dcon* routine of TopSpin, with uncertainties in line width measurements estimated to be ±8%. The MAS frequencies were in the range 3−14 kHz (stability better than ±5 Hz). For spinning sideband analysis of ^{2}H MAS NMR spectra, integral intensities were measured for spectra recorded at a MAS frequency of 3 kHz (stability better than ±2 Hz). For the γ polymorph, ^{2}H MAS NMR spectra recorded with slow MAS have partially overlapping peaks due to the $>CD_2$ and $-N^+D_3$ environments, and spectral deconvolution (as implemented in TopSpin) was employed to determine the integrated peak areas for the $>CD_2$ and $-N^+D_3$ groups. Solid-state ^{1}H and ^{2}H NMR chemical shifts were calibrated using deuterated chloroform (99.96% atom D) as a secondary reference (δ_H = 7.26 ppm relative to tetramethylsilane). To account for possible field drift over time, experimental chemical shifts were calibrated using measurements on deuterated chloroform within an hour of acquisition on the samples of glycine.

Powder X-ray diffraction data were recorded on a Bruker D8 diffractometer using Ge-monochromated Cu Kα_1 radiation with a Vånteс detector (2θ range, 4−50°; step size, 0.017°; data collection time, 25 min; foil sample holder).

^{2}H quadrupole interaction parameters were determined by analysis of the spinning sideband patterns in high-resolution solid-state ^{2}H MAS NMR spectra recorded at slow MAS frequencies. This analysis was carried out using the general purpose solid-state NMR program SPINEVOLUTION (version 3.4.2).[18] In the simulation of ^{2}H MAS NMR spectra, the "orientation" (relative to a space-fixed reference frame and specified by appropriate Euler angles) of each ^{2}H site refers to the orientation of the principal axis system of the electric field gradient (EFG) tensor at the ^{2}H nucleus. We use V^{PAS} to

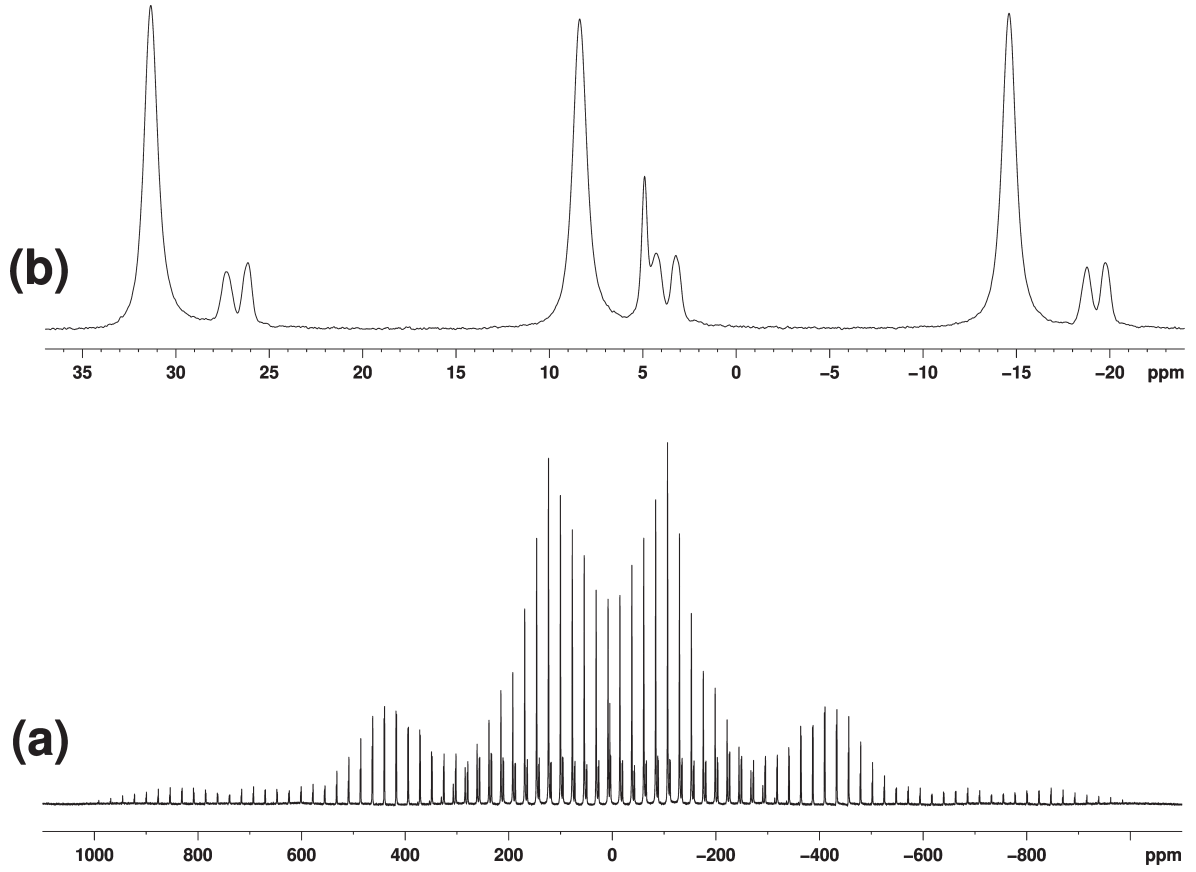

Figure 1. (a) ^{2}H MAS NMR spectrum of the α polymorph of glycine-d_5 (130.51 MHz; recycle delay, 120 s; number of scans, 4; MAS frequency, 3 kHz). (b) Expansion of the spectrum in (a) showing the isotropic peaks and first-order spinning sidebands. The peak at 4.9 ppm with no spinning sidebands is due to an unidentified impurity.[31]

denote the EFG tensor in its principal axis system. The components of V^{PAS} are taken such that $|V_{ZZ}| \geq |V_{YY}| \geq |V_{XX}|$. The quadrupole coupling constant χ is defined as eQV_{zz}/h and the asymmetry parameter η is defined as $(V_{XX} - V_{YY})/V_{ZZ}$.

Quantum-mechanical (QM) calculations to determine ^{2}H quadrupole interaction parameters were carried out using density functional theory (DFT) at the B3LYP/6-31G(df,3p) level of theory[19] using the Gaussian 09 package.[20] These calculations were carried out on molecular clusters extracted from the crystal structures of the α and γ polymorphs determined at ambient temperature from neutron diffraction data[12,13] and obtained from the CSD database (reference codes GLYCIN03[12] and GLYCIN15[13] for the α and γ polymorphs, respectively). In each case, the clusters comprised 15 glycine molecules.

Traditional QM calculations of NMR isotropic shielding (σ_{iso}) parameters were carried out using the Gaussian 09 package,[20] employing DFT at the B3LYP/6-311+G(2d,p) level[21] and the "gauge-including atomic orbital" (GIAO) method.[22] These calculations were carried out on the molecular clusters representing the α and γ polymorphs discussed above. To convert the calculated NMR isotropic shielding parameters (σ_{iso}) into calculated chemical shifts (δ_{iso}) relative to TMS, they were subtracted from the isotropic shielding parameter for tetramethylsilane (TMS) calculated at the same level of theory [B3LYP/6-311+G(2d,p), σ_{iso} = 31.8 ppm]. The geometry of TMS was optimized at the B3LYP/6-31G(d) level prior to calculation of the NMR isotropic shielding.

NMR calculations were also carried out using the CASTEP code (version 5.5)[23] based on DFT calculations for the periodic crystal structures, with planewaves and pseudopotentials employed to model the electronic wave function. All calculations used the PBE exchange correlation functional[24] with ultrasoft pseudopotentials for the atoms involved.[25] The crystal structures of the α and γ polymorphs of glycine determined from neutron diffraction data at ambient temperature[12,13] were again used in these calculations, which employed periodic boundary conditions. Two types of CASTEP calculation were considered. In the first set of calculations, geometry optimization was carried out (with all atoms allowed to relax) prior to the calculation of NMR shielding parameters. A k-point spacing of 0.04 Å^{-1} and cutoff energy of 700 eV provided a suitable minimum for both polymorphs of glycine, which were found to be almost equivalent in energy. In particular, after geometry optimization, the energy of the γ polymorph was lower than that of the α polymorph by only 0.236 kJ mol^{-1}. The optimized geometries were then used in NMR shielding calculations using the "gauge including projector augmented-wave" (GIPAW) method.[26] In the second set of calculations, the crystal structures were used directly in the NMR shielding calculations without prior geometry optimization. The calculated isotropic shielding parameters (σ_{iso}) were subtracted from the isotropic shielding value calculated for TMS at the same level of theory [PBE with ultrasoft pseudopotentials, σ_{iso} = 31.1 ppm] in order to convert them into calculated chemical shifts (δ_{iso}) relative to TMS. Prior to the NMR

shielding calculation for TMS, the geometry of a single TMS molecule placed in a 10 × 10 × 10 Å^3 cubic box was optimized using periodic boundary conditions and PBE with ultrasoft pseudopotentials. A k-point spacing of 0.07 Å^{-1} and a cutoff energy of 600 eV were used for the geometry optimization in this case, and all atoms were allowed to relax.

Natural bond orbital (NBO) analysis was carried out using Gaussian NBO version 3.1 (part of the Gaussian 09 package).[27]

4. RESULTS AND DISCUSSION

4.1. Spinning Sideband Analysis of ^{2}H MAS NMR Spectra of Glycine Polymorphs. The vast majority of reported ^{2}H NMR quadrupole interaction parameters have been derived by line shape analysis of solid-state ^{2}H NMR spectra recorded for static polycrystalline powder samples (i.e., with no sample spinning). In addition, a small number of studies involving ^{2}H NMR measurements on single-crystal samples have been reported. In principle, measurements on polycrystalline powders can provide accurate results when selectively deuterated solids are used, ensuring that the ^{2}H NMR spectrum is dominated by one crystallographically distinct ^{2}H environment. In the case of ^{2}H NMR measurements on materials with uniform levels of deuteration (e.g., fully deuterated materials or materials with natural isotopic abundances), all crystallographically inequivalent ^{2}H sites contribute to the measured ^{2}H NMR line shape, which can severely limit the ability to establish reliable information on the quadrupole interaction parameters for individual ^{2}H sites from line shape analysis. Thus, even in such simple systems as fully deuterated urea-d_4 or thiourea-d_4, there are two crystallographically inequivalent ^{2}H sites, which complicates the line shape analysis of the ^{2}H NMR spectra.[28]

In principle, high-resolution solid-state ^{2}H MAS NMR spectra recorded for polycrystalline powder samples should be able to resolve crystallographically inequivalent ^{2}H sites, provided the chemical shift differences between these sites are sufficiently large.[29] We now assess this opportunity by considering the ^{2}H MAS NMR spectrum recorded for the α polymorph of fully deuterated glycine-d_5. In particular, we use this approach to determine ^{2}H quadrupole interaction parameters for each crystallographically distinct ^{2}H site in this material, comparing our results with those reported previously from single-crystal ^{2}H NMR studies.[30] For our analysis, ^{2}H MAS NMR spectra were recorded with slow MAS (3 kHz) as the large number of spinning sidebands observed in slow MAS spectra is expected to improve the accuracy of the analysis. As shown in Figure 1, three isotropic peaks are resolved in the ^{2}H MAS NMR spectrum for the α polymorph of glycine-d_5. One isotropic peak at 8.4 ppm (the estimated accuracy for all chemical shift measurements reported here is about ±0.1 ppm) is assigned to the $-N^+D_3$ deuterons (which are rendered equivalent by dynamic reorientation of the $-N^+D_3$ group about the C−N bond), and two isotropic peaks at 3.2 and 4.3 ppm are assigned to the $>CD_2$ deuterons. Following the original notation,[12,13] the two inequivalent deuterons of the $>CD_2$ group are denoted D_4 (pro-*R*, 4.3 ppm) and D_5 (pro-*S*, 3.2 ppm). The integral intensities of 87 peaks (1 isotropic peak and 86 spinning sidebands) were measured for each of the D_4 and D_5 sites, and the integral intensities of 33 peaks (1 isotropic peak and 32 spinning sidebands) were measured for the motionally averaged $-N^+D_3$ site. For each ^{2}H site, the solid-state NMR program SPINEVOLUTION[18] was used to estimate the quadrupole coupling constant and asymmetry parameter by fitting the intensities of the isotropic peak and spinning sidebands using a Newton-type nonlinear least-squares algorithm. The results are summarized in Table 1. For comparison, the corresponding parameters determined previously[30] from single-crystal ^{2}H NMR measurements are also shown. Our results confirm that the ^{2}H quadrupole interaction parameters determined from analysis of the ^{2}H MAS NMR spectra are in good agreement with those derived from single-crystal ^{2}H NMR measurements. The ^{2}H quadrupole coupling constants show particularly good agreement, with a maximum deviation of only 1%.[33] These observations confirm that high-resolution solid-state ^{2}H MAS NMR spectra can be used successfully to determine ^{2}H quadrupole interaction parameters for crystallographically inequivalent ^{2}H sites, provided slow MAS frequencies are used.

Table 1. Quadrupole Interaction Parameters for the ^{2}H Sites in the α Polymorph of Glycine-d_5[a]

^{2}H site	δ_{iso} (ppm)	χ (kHz)	η	ref
D_5	3.1	167.6 ± 0.6	0.084 ± 0.006	this work
D_4	4.2	159.6 ± 0.7	0.058 ± 0.011	this work
$-N^+D_3$	8.4	51.1 ± 0.3[b]	0.288 ± 0.009[b]	this work
D_5	3.5[c]	169.41	0.085	30
D_4	4.3[c]	159.99	0.043	30
$-N^+D_3$	7.8[c]	50.80[b]	0.286[b]	30

[a] Determined from analysis of the ^{2}H MAS NMR spectrum and from single-crystal ^{2}H NMR measurements. [b] The quadrupole interaction parameters are averaged significantly due to reorientation of the $-N^+D_3$ group about the C−N bond. See ref 32 for values of χ and η measured at low temperatures. [c] In the single-crystal ^{2}H NMR measurements in ref 30, the isotropic chemical shifts were determined from chemical shift tensor analysis in which information from three different crystals was considered, rather than by direct measurement. See ref 33 for further details.

Using the same approach, we have also determined ^{2}H quadrupole interaction parameters for the γ polymorph of glycine-d_5. In this case, only two isotropic peaks are resolved in the ^{2}H MAS NMR spectrum (Figure 2), assigned to the $-N^+D_3$ deuterons (8.8 ppm) and the $>CD_2$ deuterons (3.2 ppm). The integral intensities of 27 and 87 peaks (isotropic peak plus spinning sidebands) were measured for the $-N^+D_3$ and $>CD_2$ groups, respectively, and were used in our analysis of the intensity distribution of the spinning sidebands. The ^{2}H quadrupole interaction parameters established from fitting the measured sideband intensity patterns are χ = 165.7 ± 0.5 kHz and η = 0.061 ± 0.006 for the $-N^+D_3$ deuterons, and χ = 50.2 ± 0.7 kHz and η = 0.291 ± 0.017 for the $>CD_2$ deuterons.

As structures of organic materials determined from neutron diffraction data (which provide accurate information on H atom positions) at ambient temperature are relatively scarce, other methods may be needed to establish structural correlations of NMR parameters in order to extend applications of ^{2}H MAS NMR. Quantum-mechanical (QM) methods are useful in this regard (e.g., for refining H atom positions starting from structures determined from X-ray diffraction data and/or for calculating NMR parameters for structures in the absence of motion), although the ability of computational methods to *accurately* reproduce experimental data measured at ambient temperature is always a matter of significant concern. The availability of accurate structural data for the α and γ polymorphs of glycine at ambient temperature, determined from neutron diffraction data, is such that these structures can be used

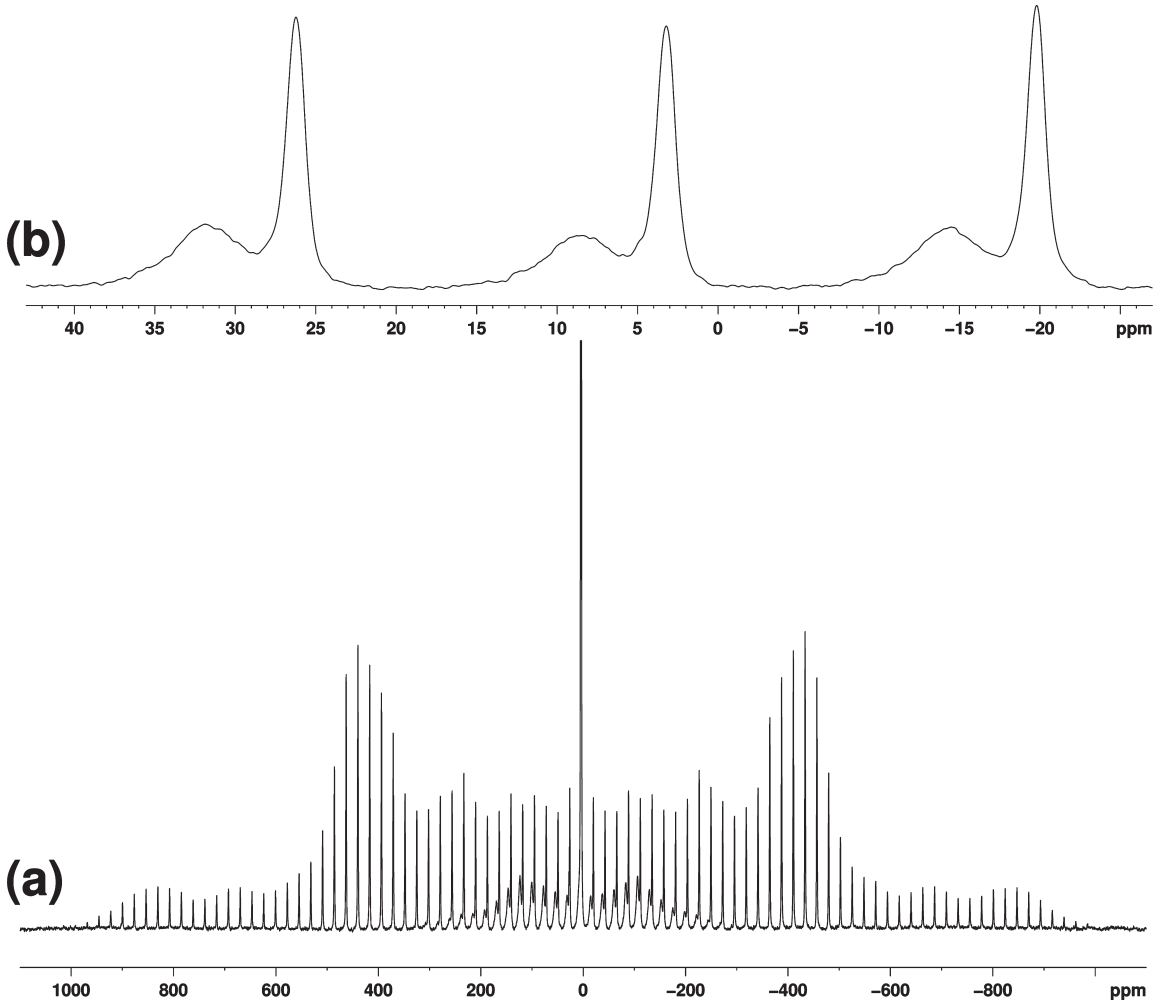

Figure 2. (a) ^{2}H MAS NMR spectrum of the γ polymorph of glycine-d_5 (130.51 MHz; recycle delay, 300 s; number of scans, 16; MAS frequency, 3 kHz). (b) Expansion of the ^{2}H CPMAS NMR spectrum of the γ polymorph of glycine-d_5 showing the isotropic peaks and first-order spinning sidebands (130.51 MHz; recycle delay, 150 s; number of scans, 240; CP contact time, 1 ms; MAS frequency, 3 kHz). Integral intensities of spinning sidebands measured from (a) were used to determine the ^{2}H quadrupole interaction parameters. As a peak due to an unidentified impurity is present in (a), the integral intensities of the isotropic peaks due to glycine-d_5 in (a) were estimated using the relative integral intensities of the isotropic and first-order sidebands shown in the ^{2}H CPMAS NMR spectrum in (b). Cross-polarization allows the peak due to the impurity to be fully suppressed in this case.[31]

directly in QM calculations without geometry optimization, focusing here on the calculation of ^{2}H quadrupole interaction parameters (χ and η). Experimentally determined values of χ and η for the >CD_2 deuterons in the α and γ polymorphs of glycine are also available at ambient temperature from single-crystal ^{2}H NMR and ^{2}H MAS NMR measurements (Table 1). However, with a few exceptions,[10m,19,34] the reliability of QM methods for predicting ^{2}H quadrupole interaction parameters has not been examined extensively. In a recent report by Griffin et al.,[10m] good agreement between calculated and experimental parameters was noted for OD-brucite, although the calculated ^{2}H quadrupole coupling constant was overestimated by ~31 kHz (~12%) compared to the experimental value. This level of accuracy may not be sufficient in the case of polymorphic systems, which are expected to exhibit relatively small differences in NMR parameters. The approach described by Bailey[19] is promising in this regard, as it shows an rms difference of 3.2 kHz (2.7%) between calculated and experimental ^{2}H quadrupole coupling constants, although this result was obtained for calculations on isolated molecules. Here, we extend this approach to the solid state by using a molecular cluster that preserves, for the central molecule in the cluster, the set of intermolecular interactions present in the solid state.

For our calculations of the ^{2}H quadrupole interaction parameters for the α and γ polymorphs of glycine, we have chosen DFT B3LYP/6-31G(df,3p) calculations of the central glycine molecule in 15-molecule clusters extracted from the known crystal structures at ambient temperature (Figure 3). The geometries of these clusters were used without further optimization in the DFT calculations. To convert the electric field gradient tensor components in the principal axis system into ^{2}H quadrupole coupling tensor components, the scaling factor 636.5 kHz/a.u. reported by Bailey[19] was used. The calculated ^{2}H quadrupole interaction parameters are: D_4 (α polymorph), χ = 176.9 kHz, η = 0.0985; D_5 (α polymorph), χ = 167.1 kHz, η = 0.0363; D_4 (γ polymorph), χ = 162.5 kHz, η = 0.1062; D_5 (γ polymorph), χ = 159.9 kHz, η = 0.0465. Comparison with the experimental values (Table 1) suggests that the DFT calculations at the B3LYP/6-31G(df,3p) level reproduce adequately the structural dependence of the ^{2}H quadrupole interaction parameters for both the α and γ polymorphs. In particular, the DFT

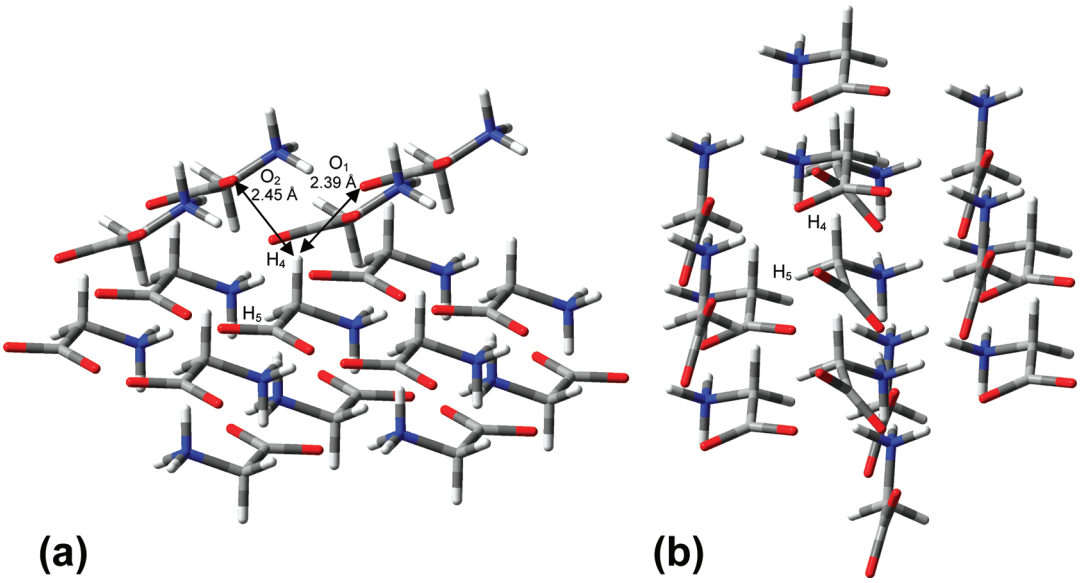

Figure 3. The 15-molecule clusters of glycine extracted from the crystal structures[12,13] of (a) the α polymorph and (b) the γ polymorph, as used in our DFT calculations. The methylene hydrogen atoms H_4 (pro-*R*) and H_5 (pro-*S*) in the central glycine molecule are identified in each case. For the α polymorph, intermolecular $H_4\cdots O$ close contacts (2.39 and 2.45 Å) revealed by the NBO analysis (see text) are highlighted by arrows.

calculations confirm that: (i) for each polymorph, both χ and η are higher for the D_5 environment than the D_4 environment, and (ii) the *difference* between the values of χ for the D_5 and D_4 environments is significantly lower for the γ polymorph (calculated, 2.6 kHz; experimental, 0 kHz) than the α polymorph (calculated, 9.8 kHz; experimental, 8.0 kHz). The significant difference between the values of χ for the D_4 and D_5 environments in the α polymorph may be attributed to the fact that D_4 [H(4) in the original notation[12]] has two close oxygen atom neighbors (H···O, 2.39 Å, C−H···O, 137.4°; H···O, 2.45 Å, C−H···O, 140.0°), whereas D_5 [H(5) in the original notation[12]] has no close contacts of this type. It is well-known that the magnitude of the ^{2}H quadrupole coupling constant decreases when a deuteron is involved in a hydrogen bonding interaction, and this fact has been exploited previously in structural elucidation.[35] The influence of the intermolecular proximity of these two oxygen atoms on the ^{1}H NMR chemical shifts for the α polymorph (discussed below) is also indicative of significant $C-H_4\cdots O$ interactions.

4.2. Sensitivity of ^{2}H MAS NMR Spectra to Reorientational Motions. The ^{2}H MAS NMR spectra for the α and γ polymorphs of glycine-d_5 (Figures 1 and 2) reveal significant differences in the relative intensities of the spinning sideband manifolds for the $>CD_2$ and $-N^+D_3$ groups. In particular, for the γ polymorph, the relative intensity of the spinning sideband manifold for the $-N^+D_3$ deuterons is significantly *lower* than that for the CD_2 deuterons (Figure 2), whereas for the α polymorph, the relative intensity of the spinning sideband manifold for the $-N^+D_3$ deuterons is significantly *higher* than that for the CD_2 deuterons (Figure 1). Furthermore, both the isotropic peak and spinning sidebands for the $-N^+D_3$ deuterons are significantly broader for the γ polymorph (half-height line width $\Delta\nu_{1/2} \approx 650$ Hz) than the α polymorph ($\Delta\nu_{1/2} \approx$ 100 Hz). Similar differences in the distribution of intensities and linewidths between the α and γ polymorphs are also observed in the ^{2}H MAS NMR spectra recorded at MAS frequency 14 kHz (Figure 4). Previously, it has been suggested[1] that the line broadening observed in the ^{2}H MAS NMR spectrum of the γ polymorph may be due to the frequency of the reorientational motion of the $-N^+D_3$ group[36,37] approaching the same order of magnitude as the static ^{2}H quadrupole coupling constant.

Here, we have carried out simulations of ^{2}H MAS NMR spectra in order to assess how the shape of the spinning sideband manifold depends on the reorientational jump frequency (κ) of the $-N^+D_3$ group, assuming a three-site jump motion (Figure 5). These simulations confirm our previous assumption that line broadening in ^{2}H MAS NMR spectra may be indicative of reorientational frequencies in the intermediate motion regime with respect to the ^{2}H NMR time scale. Remarkably, the simulated ^{2}H MAS NMR spectra show a dependence ($\Delta\nu_{1/2}$ vs κ) in the range $\kappa \approx 10^2-10^9$ s^{-1} (Figure 5), which is significantly wider than the motional frequency range accessible via analysis of wide-line ^{2}H NMR quadrupole echo lineshapes ($\kappa \approx 10^4-10^8$ s^{-1}). The simulated ^{2}H MAS NMR spectrum that reproduces most closely the experimentally measured line width of the isotropic peak for the γ polymorph ($\Delta\nu_{1/2} \approx 310$ Hz at MAS frequency 14 kHz) is that simulated for $\kappa = 10^{7.5}$ s^{-1} (Figure 5m), for which $\Delta\nu_{1/2} \approx$ 331 Hz. However, accurate estimation of κ would require knowledge of the intrinsic line width and corrections for any other sources of line broadening. Without such corrections, the reorientational jump frequency of the $-N^+D_3$ group in the γ polymorph is estimated (from the ^{2}H MAS NMR simulations in Figure 5) to be $\kappa > 10^{7.5}$ s^{-1}. For comparison, from the temperature dependence of the jump frequency of the $-N^+D_3$ group established[37] from analysis of wide-line ^{2}H NMR lineshapes between 183 and 258 K (and extrapolating to higher temperatures on the assumption of Arrhenius behavior), the value of κ at 298 K for the γ polymorph of glycine-d_3 ($D_3N^+CH_2COO^-$) is predicted to be 3.6×10^8 s^{-1}.

In terms of natural-abundance ^{2}H MAS NMR measurements, our simulations suggest that severe broadening of the ^{2}H MAS NMR signal may occur in the intermediate motion regime. In particular, in the simulated spectra calculated for $\kappa = 10^{4.5}$ s^{-1} and $\kappa = 10^5$ s^{-1} (Figures 5g and 5h), the intensity is lower by a

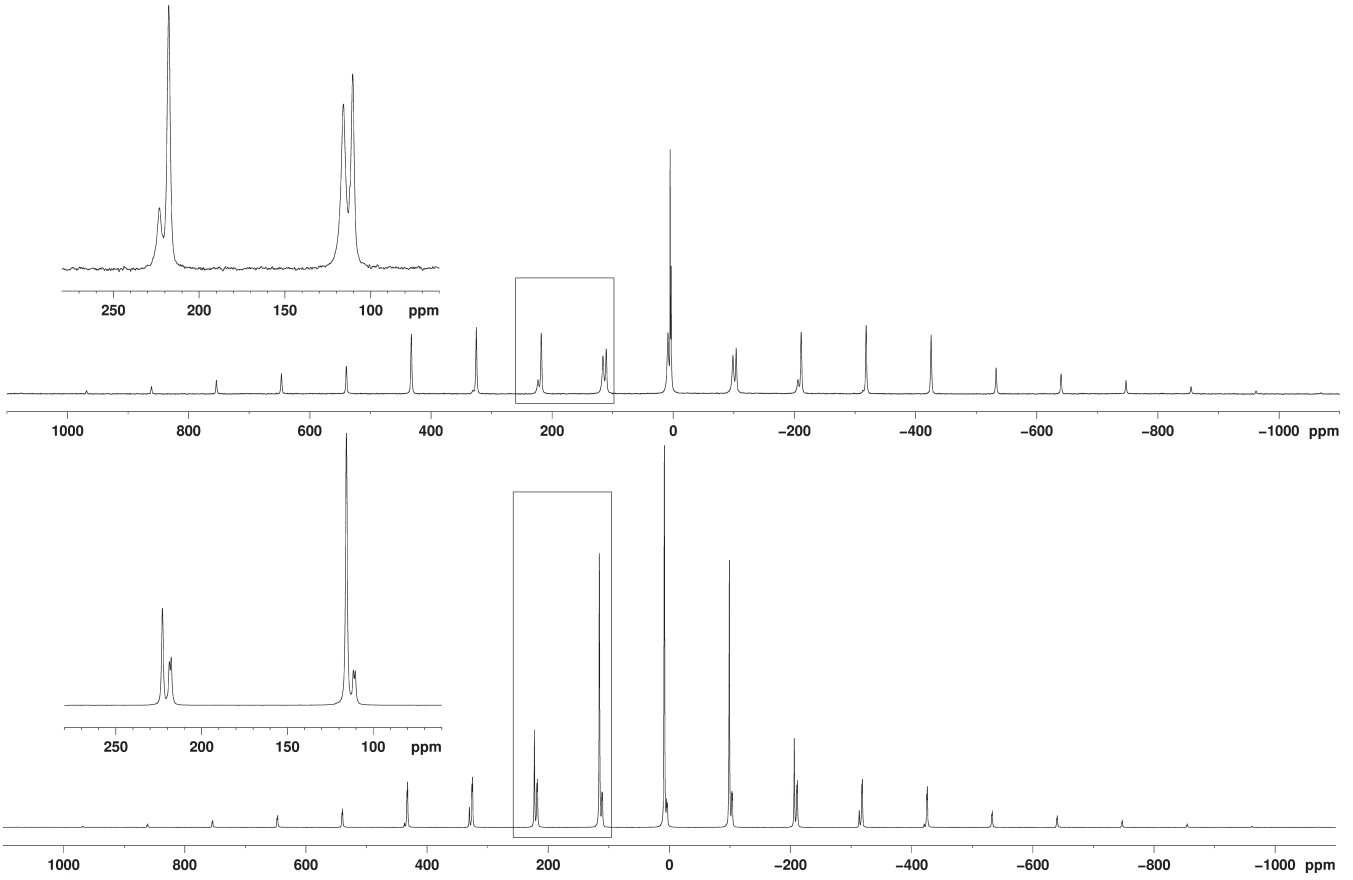

Figure 4. (a) ^{2}H MAS NMR spectrum of the α polymorph of glycine-d_5 (130.51 MHz; recycle delay, 20 s; number of scans, 8; MAS frequency, 14 kHz). (b) ^{2}H MAS NMR spectrum of the γ polymorph of glycine-d_5 (130.51 MHz; recycle delay, 120 s; number of scans, 6; MAS frequency 14 kHz). The expansions of the spectra show the first-order and second-order spinning sidebands.

factor of ∼1400 than the "static" ^{2}H MAS NMR spectrum (Figure 5a). From the dependence of spectral intensity on the frequency of the reorientational motion shown in Figure 5, it is clear that the most suitable conditions for recording high-resolution solid-state ^{2}H MAS NMR spectra for materials with natural isotopic abundances is either the "static" motion regime (Figure 5a) or the rapid motion regime (Figures 5p−r).

4.3. ^{1}H Chemical Shifts from ^{2}H MAS NMR Spectra and QM Calculations. For the α polymorph of glycine-d_5, there is a relatively large difference of 1.1 ppm between the ^{2}H NMR chemical shifts for the two deuterons of the >CD_2 group (D_4, 4.2 ppm; D_5, 3.1 ppm). For the γ polymorph, on the other hand, distinct signals due to the corresponding two deuterons are not resolved in the ^{2}H MAS NMR spectrum (3.2 ppm for both D_4 and D_5). ^{2}H (and ^{1}H) NMR chemical shifts are determined from ^{2}H NMR peak maximum positions by taking into account the second-order shift, determined to be +0.115 ppm at 20 T for the >CD_2 deuterons,[1] where "+" corresponds to a high-frequency shift of the peak maximum in the ^{2}H NMR spectrum relative to that in the ^{1}H NMR spectrum. Due to fast motional averaging (see Table 1), the second-order shift is reduced to +0.013 ppm at 20 T for the $-N^+D_3$ deuterons. Chemical shifts determined in this way (Table 2) are within ±0.1 ppm of the values determined from ^{1}H MAS NMR spectra for the α and γ polymorphs of glycine-d_5. No corrections were made due to deuterium isotope effects on ^{1}H chemical shifts (about −30 ppb over two bonds).[38]

Following many successful applications of quantum mechanical chemical shift calculations for solution-state and gas-phase NMR, we explore here the relative accuracy of similar calculations in the solid state, specifically for distinguishing different polymorphic forms and for relating the observed differences in NMR parameters to structural differences between the two polymorphs. Recently, Stievano et al. reported[39] calculations of chemical shifts for polymorphs of glycine. In the case of ^{1}H chemical shifts, the level of agreement with experimental data was relatively poor. In particular, for the γ polymorph, the calculated values for the structure determined by neutron diffraction were 1.4 and 1.8 ppm, which differ significantly from the experimental value of 3.2 ppm. Here, we consider two types of calculations. First, we consider traditional QM calculations based on the "gauge-including atomic orbital" (GIAO) method, similar to those reported for the solution state and gas phase. For these calculations, we used 15-molecule clusters extracted from the crystal structures of the α and γ polymorphs of glycine at ambient temperature (Figure 3), and the ^{1}H NMR chemical shifts for the central glycine molecule in these clusters were calculated at the B3LYP/6-311+G(2d,p) level of theory. Inclusion of all nearest-neighbor glycine molecules around the central molecule in the cluster is expected to allow for any significant influence of intermolecular interactions on the calculated NMR properties. The results are summarized in Table 2.

In addition to traditional QM calculations, we have also considered the "gauge including projected augmented wave" (GIPAW) method, which enables the calculation of all-electron

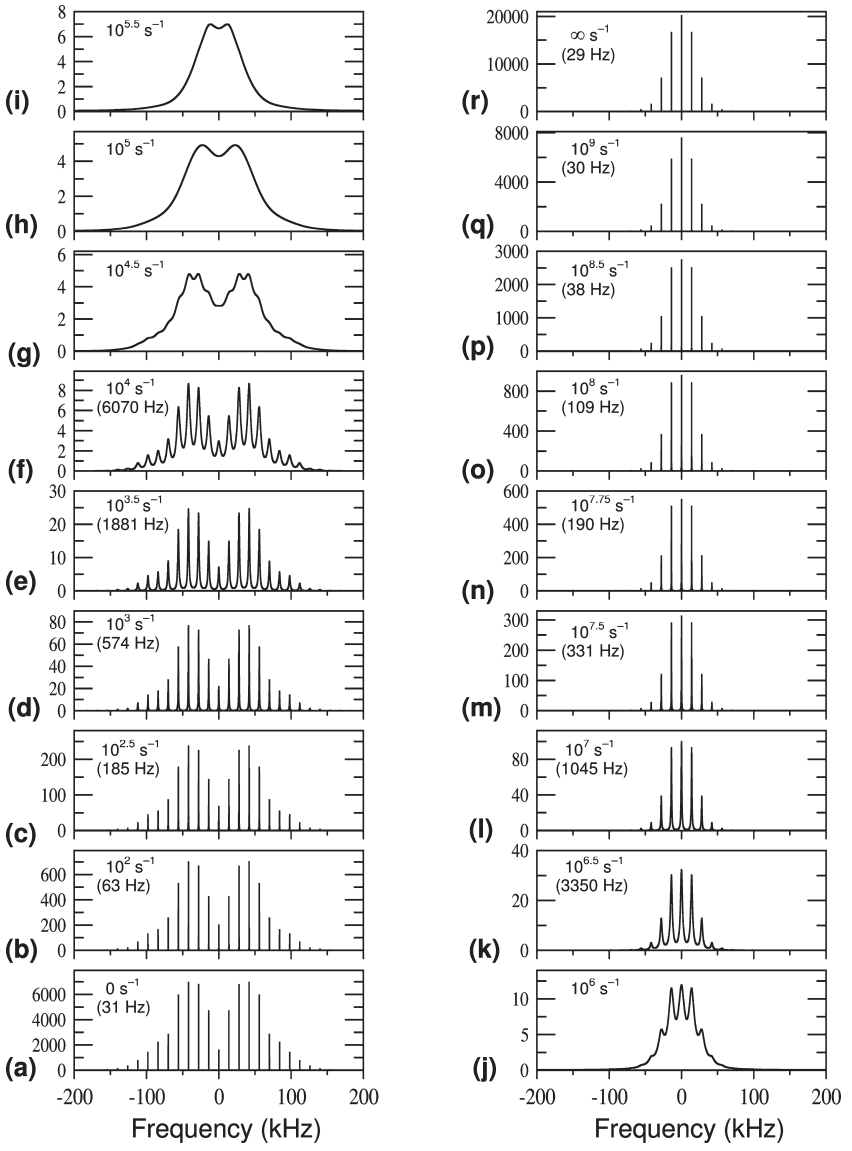

Figure 5. Simulated ^{2}H MAS NMR spectra for reorientation of the $-N^+D_3$ group, modeled as a three-site jump motion about the C−N bond. The spectra were calculated using SPINEVOLUTION,[18] with the following parameters: ^{2}H quadrupole coupling constant, 160 kHz; ^{2}H asymmetry parameter, 0; isotropic ^{2}H chemical shift, 0 ppm; MAS frequency, 14 kHz; line broadening, 5 Hz; Larmor frequency, 130.51 MHz. The ^{2}H quadrupole coupling constants and asymmetry parameters (χ, η) used for the three inequivalent $-N^+D_3$ sites were those measured at 77 K for the γ polymorph of glycine-d_5 (145.3 kHz, 0.055; 159.0 kHz, 0.044; 174.7 kHz, 0.034).[32] The principal component of the ^{2}H electric field gradient tensor is assumed to be parallel to the N−D bond, which forms an angle of 109.47° with the reorientation axis. The reorientational jump frequencies (κ) and the measured half-height line widths of the isotropic peak ($\Delta\nu_{1/2}$, in brackets) are also shown.

NMR parameters in solids and uses periodic boundary conditions in order to represent the complete periodic crystal structure.[26] The GIPAW method relies on the plane wave pseudopotential formalism of DFT and avoids the use of the cluster approximation. As shown previously,[40] geometry optimization of crystal structures determined from diffraction data may sometimes lead to improved correlation between calculated ^{13}C shielding parameters and experimental ^{13}C chemical shifts. We therefore considered two types of GIPAW calculation, both with geometry optimization and without geometry optimization. The results are summarized in Table 2.

For the $-N^+H_3$ group, GIAO and GIPAW calculations with no prior geometry optimization show better agreement with the experimentally measured ^{1}H NMR chemical shifts than GIPAW calculations with geometry optimization (Table 2). However, in the case of the $-N^+H_3$ group, which is known to undergo large amplitude motion at ambient temperature, prediction of properties (including chemical shifts) by QM calculations may show relatively large deviations from experimental results due to large anharmonicity effects.[41] In the following discussion, we therefore focus on comparison of the chemical shifts for the $>CH_2$ group, as this group does not undergo large amplitude motions at ambient temperature in either the α or γ polymorph of glycine, as supported by the measured ^{2}H quadrupole interaction parameters (see Section 4.1 and Table 1 above). For the α polymorph, both GIAO and GIPAW calculations show satisfactory agreement with the experimentally measured ^{1}H NMR chemical shifts (see Table 2). The GIPAW calculation with no prior

Table 2. Calculated and Experimental ^{1}H NMR Chemical Shifts (δ_{iso}/ppm) for the CH_2 Group in the α and γ Polymorphs of Glycine

polymorph	^{1}H environment	experiment	calcd GIAO B3LYP	calcd GIPAW PBE[a]	calcd GIPAW PBE[b]
α	H_4	4.2	4.7	4.7	4.3
α	H_5	3.1	3.5	3.5	3.3
α	$-N^+H_3$ (aver.)	8.4	8.1	9.9	8.5
α	$-N^+H_3$		10.5, 8.1, 5.6	12.5, 10.1, 7.1	11.3, 8.4, 5.9
γ	H_4	3.2	3.7	3.3	3.4
γ	H_5	3.2	4.0	3.5	3.7
γ	$-N^+H_3$ (aver.)	8.8	9.1	9.9	9.5
γ	$-N^+H_3$		10.1, 9.2, 8.1	11.9, 10.0, 7.9	11.2, 9.2, 8.1

[a] Geometry optimization was performed on the atomic coordinates in the crystal structure prior to the NMR calculations, with the unit cell parameters held constant. [b] The crystal structures determined from neutron diffraction data were used directly in the NMR calculations without geometry optimization.

geometry optimization shows very good quantitative agreement with the experimental values. For the γ polymorph, however, GIPAW calculations perform better than GIAO calculations, although in terms of the difference between the chemical shifts for the two protons in the $>CH_2$ group [$\Delta\delta_{iso} = \delta_{iso}(H_4) - \delta_{iso}(H_5)$], both types of calculation reproduce the experimental values equally well. Overall, for the four methylene ^{1}H NMR chemical shift values in the two polymorphs, the mean absolute deviations from the experimental values are 0.55 ppm for the GIAO calculation, and 0.33 and 0.25 ppm for the GIPAW calculations with and without geometry optimization, respectively.

An additional advantage of QM calculations is that natural bond orbital (NBO)[27,42] analysis can be carried out to assess the strengths of intermolecular interactions present, allowing the significant noncovalent interactions to be identified. Such insights are important, as there are typically a large number of noncovalent interactions involving the site of a given nucleus in a crystal structure, such that it may be difficult to discriminate the important structural factors that influence the chemical shift. In the present work, NBO analysis was carried out at the B3LYP/6-311+G(2d,p) level for the molecular cluster used in the traditional QM calculations (Figure 3). For the central glycine molecule in the cluster representing the α polymorph, second order perturbation theory analysis of the Fock matrix in the NBO basis (which is used to estimate the energies of delocalization of electrons from filled NBOs into empty NBOs) showed three intermolecular $n_0 \rightarrow \sigma^*(C-H_4)$ delocalizations from lone pairs on oxygen atoms O_1 and O_2 (Figure 3) into the $C-H_4$ antibond, with stabilization energies greater than 0.5 kcal mol^{-1} (specifically, 0.52, 0.89, and 1.15 kcal mol^{-1}). For comparison, the largest stabilization energy for other intermolecular delocalizations is only 0.23 kcal mol^{-1} for the $C-H_5$ antibond in the α polymorph, 0.21 kcal mol^{-1} for the $C-H_4$ antibond in the γ polymorph and 0.45 kcal mol^{-1} for the $C-H_5$ antibond in the γ polymorph. Relatively strong intermolecular $n_0 \rightarrow \sigma^*(C-H)$ delocalization into the $C-H_4$ antibond in the α polymorph leads to a decrease in the electron density on H_4 (calculated natural charge +0.27 au) compared to H_5 in the α polymorph (+0.22 au) and to H_4 and H_5 in the γ polymorph (+0.23 au and +0.24 au respectively).[43] Thus, the high-frequency shift observed for H_4 in the α polymorph (Table 2) can be attributed to intermolecular $C-H\cdots O$ close contacts. These results suggest that, in spite of the relatively narrow span of ^{1}H NMR chemical shifts (ca. 10 ppm), computation of ^{1}H NMR chemical shifts can successfully distinguish small differences in chemical shifts between polymorphs and, furthermore, can provide insights into the reasons underlying differences in chemical shifts induced by differences in molecular geometry and crystal packing.

5. CONCLUDING REMARKS

To assess the depth and quality of information provided by high-resolution solid-state ^{2}H MAS NMR, we have carried out detailed studies on the α and γ polymorphs of fully deuterated glycine (glycine-d_5). In the first instance, analysis of spinning sideband patterns was used to determine the ^{2}H quadrupole interaction parameters. The results show good agreement with the corresponding parameters determined from single-crystal ^{2}H NMR measurements. In particular, the maximum deviation in ^{2}H quadrupole coupling constants determined by these two approaches is only 1%. These findings suggest that the resolution provided by ^{2}H MAS NMR may, in principle, be sufficient for accurate determination of ^{2}H quadrupole interaction parameters without the need to grow suitable single crystals for single-crystal ^{2}H NMR studies and without the requirement to have suitable equipment for carrying out single-crystal NMR measurements.

As demonstrated here, solid-state ^{2}H MAS NMR spectra are sensitive to dynamic processes and may, therefore, be exploited to provide insights on molecular motion in solids. Thus, the dynamics of the $-N^+D_3$ group in the α and γ polymorphs of glycine-d_5 allows an assessment of the effect of the rate of molecular motion on the measured spectra. From analysis of simulated ^{2}H MAS NMR sideband patterns as a function of reorientational jump frequency (κ) for the $-N^+D_3$ group, observed differences in the experimental ^{2}H MAS NMR spectra for the α and γ polymorphs can be attributed directly to differences in the rate of reorientation of the $-N^+D_3$ group. The measured line widths and relative intensities of spinning sideband manifolds suggest that the rate of reorientation of the $-N^+D_3$ group is much faster in the α polymorph than the γ polymorph, in agreement with results from previous studies and the suggestion that the $-N^+H_3$ group is engaged in stronger hydrogen bonding in the γ polymorph. Spectral simulations show significant broadening of the ^{2}H MAS NMR signal in the intermediate motion regime, suggesting that deuterons undergoing reorientation at rates in the range $\kappa \approx 10^4 - 10^6$ s^{-1} are likely to be undetectable in ^{2}H MAS NMR spectra for materials with natural isotopic abundances. Remarkably, isotropic line widths in simulated ^{2}H MAS NMR spectra exhibit a significant dependence on the reorientational jump

frequency across the range $\kappa \approx 10^2-10^9$ s^{-1}, which is significantly wider than the range of motional frequencies that are accessible via analysis of wide-line ^{2}H NMR quadrupole echo lineshapes ($\kappa \approx 10^4-10^8$ s^{-1}).

Importantly, ^{2}H NMR chemical shifts can be readily measured from ^{2}H MAS NMR spectra but are not accessible from wide-line ^{2}H NMR spectra. Furthermore, the measured data provide access to ^{1}H NMR chemical shifts, the structural dependence of which has been widely explored in the past. Here, the ^{1}H NMR chemical shifts for the α and γ polymorphs of glycine have been determined from our ^{2}H MAS NMR results. However, as NMR parameters depend on a large number of factors with various origins, their interpretation is not necessarily straightforward. We have therefore investigated the opportunity to exploit QM calculations of ^{2}H quadrupole interaction parameters and ^{1}H chemical shifts in order to reveal the structural dependence of these parameters. Our results suggest that the existence of two short intermolecular C−H···O contacts for one H atom (specifically H_4) of the >CH_2 group in the α polymorph of glycine has a significant influence on the ^{2}H quadrupole coupling constant and the ^{1}H chemical shift for this site.

We have also explored the advantages provided by QM natural bond orbital analysis for identifying relatively strong intermolecular interactions in the solid state. For the H_4 atom in the >CH_2 group of the α polymorph, three intermolecular $n_O \rightarrow \sigma^*(C-H_4)$ delocalizations from lone pairs on oxygen atoms of neighboring molecules are associated with stabilization energies greater than 0.5 kcal mol^{-1}, while in contrast, the intermolecular delocalization is significantly weaker for the H_5 site in the α polymorph and for both H atoms in the >CH_2 group of the γ polymorph.

AUTHOR INFORMATION

Corresponding Author

*E-mail: a.e.aliev@ucl.ac.uk; harriskdm@cardiff.ac.uk.

ACKNOWLEDGMENT

The UK 850 MHz Solid-State NMR Facility used in this research was funded by EPSRC and BBSRC, as well as the University of Warwick, including via part funding through Birmingham Science City Advanced Materials Projects 1 and 2 supported by Advantage West Midlands (AWM) and the European Regional Development Fund (ERDF).

REFERENCES

(1) Aliev, A. E.; Mann, S. E.; Iuga, D.; Hughes, C. E.; Harris, K. D. M. *J. Phys. Chem. A* **2011**, *115*, 5568.

(2) Maricq, M.; Waugh, J. S. *Chem. Phys. Lett.* **1977**, *47*, 327.

(3) Aliev, A. E.; Harris, K. D. M.; Apperley, D. C. *Chem. Phys. Lett.* **1994**, *226*, 193.

(4) Mizuno, T.; Nemoto, T.; Tansho, M.; Shimizu, T.; Ishii, H.; Takegoshi, K. *J. Am. Chem. Soc.* **2006**, *128*, 9683.

(5) Reichert, D.; Olender, Z.; Poupko, R.; Zimmermann, H.; Luz, Z. *J. Chem. Phys.* **1993**, *98*, 7699.

(6) Poupko, R.; Olender, Z.; Reichert, D.; Luz, Z. *J. Magn. Reson., Ser. A* **1994**, *106*, 113.

(7) Gérardy-Montouillout, V.; Malveau, C.; Tekely, P.; Olender, Z.; Luz, Z. *J. Magn. Reson., Ser. A* **1996**, *123*, 7.

(8) Malveau, C.; Tekely, P.; Canet, D. *Solid State Nucl. Magn. Reson.* **1997**, *7*, 271.

(9) De Laeter, J. R.; Böhlke, J. K.; De Bièvre, P.; Hidaka, H.; Peiser, H. S.; Rosman, K. J. R.; Taylor, P. D. P. *Pure Appl. Chem.* **2003**, *75*, 683.

(10) (a) Griffin, R. G. *Methods Enzymol.* **1981**, *72*, 108. (b) Alam, T. M.; Drobny, G. P. *Chem. Rev.* **1991**, *91*, 1545. (c) Ripmeester, J. A.; Ratcliffe, C. I. Solid-State NMR Studies of Inclusion Compounds. In *Inclusion Compounds*; Attwood, J. L., Davies, J. E. D., MacNicol, D. D., Eds.; Oxford University Press: Oxford, 1991; Vol. 5, p 37; (d) Hoatson, G. L.; Vold, R. L. *NMR Basic Principles and Progress*; Springer-Verlag: Berlin, 1994; Vol. 32, pp 3− 67; (e) Aliev, A. E.; Smart, S. P.; Harris, K. D. M. *J. Mater. Chem.* **1994**, *4*, 35. (g) Harris, K. D. M.; Aliev, A. E. *Chem. Brit.* **1995**, *31*, 132. (h) Aliev, A. E.; Harris, K. D. M.; Shannon, I. J.; Glidewell, C.; Zakaria, C. M.; Schofield, P. A. *J. Phys. Chem.* **1995**, *99*, 12008. (i) Aliev, A. E.; Smart, S. P.; Shannon, I. J.; Harris, K. D. M. *J. Chem. Soc., Faraday Trans.* **1996**, *92*, 2179. (j) Aliev, A. E.; Harris, K. D. M. *J. Phys. Chem. A* **1997**, *101*, 4541. (k) Cutajar, M.; Ashbrook, S. E.; Wimperis, S. *Chem. Phys. Lett.* **2006**, *423*, 276. (l) Hogg, N. H. M.; Boulton, P. J. T.; Zorin, V. E.; Harris, R. K.; Hodgkinson, P. *Chem. Phys. Lett.* **2009**, *475*, 58. (m) Griffin, J. M.; Miller, A. J.; Berry, A. J.; Wimperis, S.; Ashbrook, S. E. *Phys. Chem. Chem. Phys.* **2010**, *12*, 2989.

(11) (a) Albrecht, G.; Corey, R. B. *J. Am. Chem. Soc.* **1939**, *61*, 1087. (b) Iitaka, Y. *Acta Crystallogr.* **1960**, *13*, 35. (c) Iitaka, Y. *Acta Crystallogr.* **1961**, *14*, 1. (d) Drebushchak, T. N.; Boldyreva, E. V.; Shutova, E. S. *Acta Crystallogr., Sect. E* **2002**, *58*, o634.

(12) Jönsson, P.-G.; Kvick, Å. *Acta Crystallogr., Sect. B* **1972**, *28*, 1827.

(13) Kvick, Å.; Canning, W. M.; Koetzle, T. F.; Williams, G. J. B. *Acta Crystallogr., Sect. B* **1980**, *36*, 115.

(14) (a) Perlovich, G. L.; Hansen, L. K.; Bauer-Brandl, A. *J. Therm. Anal. Cal.* **2001**, *66*, 699. (b) Boldyreva, E. V.; Drebushchak, V. A.; Drebushchak, T. N.; Paukov, I. E.; Kovalevskaya, Y. A.; Shutova, E. S. *J. Therm. Anal. Cal.* **2003**, *73*, 419. (c) Boldyreva, E. V.; Drebushchak, V. A.; Drebushchak, T. N.; Paukov, I. E.; Kovalevskaya, Y. A.; Shutova, E. S. *J. Therm. Anal. Cal.* **2003**, *73*, 409.

(15) (a) Bhat, M. N.; Dharmaprakash, S. M. *J. Cryst. Growth* **2002**, *242*, 245. (b) Garetz, B. A.; Matic, J.; Myerson, A. S. *Phys. Rev. Lett.* **2002**, *89*, 175501. (c) Aber, J. E.; Arnold, S.; Garetz, B. A.; Myerson, A. S. *Phys. Rev. Lett.* **2005**, *94*, 145503. (d) He, G. W.; Bhamidi, V.; Wilson, S. R.; Tan, R. B. H.; Kenis, P. J. A.; Zukoski, C. F. *Cryst. Growth Des.* **2006**, *6*, 1746. (e) Xu, M.; Harris, K. D. M. *J. Phys. Chem. B* **2007**, *111*, 8705.

(16) (a) Myerson, A. S.; Lo, P. Y. *J. Cryst. Growth* **1990**, *99*, 1048. (b) Shimon, L. J. W.; Vaida, M.; Addadi, L.; Lahav, M.; Leiserowitz, L. *J. Am. Chem. Soc.* **1990**, *112*, 6215. (c) Gidalevitz, D.; Feidenhans'l, R.; Matlis, S.; Similgies, D. F.; Christensen, M. J.; Leiserowitz, L. *Angew. Chem., Int. Ed.* **1997**, *36*, 955. (d) Towler, C. S.; Davey, R. J.; Lancaster, R. W.; Price, C. J. *J. Am. Chem. Soc.* **2004**, *126*, 13347. (e) Weissbuch, I.; Torbeev, V. Y.; Leiserowitz, L.; Lahav, M. *Angew. Chem., Int. Ed.* **2005**, *44*, 3226. (f) Yu, L.; Huang, J.; Jones, K. J. *J. Phys. Chem. B* **2005**, *109*, 19915. (g) Huang, J.; Stringfellow, T. C.; Yu, L. *J. Am. Chem. Soc.* **2008**, *130*, 13973. (h) Hughes, C. E.; Hamad, S.; Harris, K. D. M.; Catlow, C. R. A.; Griffiths, P. C. *Faraday Discuss.* **2007**, *136*, 71. (i) Hughes, C. E.; Harris, K. D. M. *J. Phys. Chem. A* **2008**, *112*, 6808. (j) Hughes, C. E.; Harris, K. D. M. *New J. Chem.* **2009**, *33*, 713. (k) Hughes, C. E.; Harris, K. D. M. *Chem. Commun.* **2010**, *46*, 4982. (l) Yu, L. *Acc. Chem. Res.* **2010**, *43*, 1257.

(17) Fung, B. M.; Khitrin, A. K.; Ermolaev, K. *J. Magn. Reson.* **2000**, *142*, 97.

(18) Vershtort, M.; Griffin, R. G. *J. Magn. Reson.* **2006**, *178*, 248.

(19) Bailey, W. C. *J. Mol. Spectrosc.* **1998**, *190*, 318.

(20) Frisch, M. J.; Trucks, G. W.; Schlegel, H. B.; Scuseria, G. E.; Robb, M. A.; Cheeseman, J. R.; Scalmani, G.; Barone, V.; Mennucci, B.; Petersson, G. A.; Nakatsuji, H.; Caricato, M.; Li, X.; Hratchian, H. P.; Izmaylov, A. F.; Bloino, J.; Zheng, G.; Sonnenberg, J. L.; Hada, M.; Ehara, M.; Toyota, K.; Fukuda, R.; Hasegawa, J.; Ishida, M.; Nakajima, T.; Honda, Y.; Kitao, O.; Nakai, H.; Vreven, T.; Montgomery, J. A., Jr.; Peralta, J. E.; Ogliaro, F.; Bearpark, M.; Heyd, J. J.; Brothers, E.; Kudin, K. N.; Staroverov, V. N.; Kobayashi, R.; Normand, J.; Raghavachari, K.; Rendell, A.; Burant, J. C.; Iyengar, S. S.; Tomasi, J.; Cossi, M.; Rega, N.; Millam, N. J.; Klene, M.; Knox, J. E.; Cross, J. B.; Bakken, V.; Adamo, C.; Jaramillo, J.; Gomperts, R.; Stratmann, R. E.; Yazyev, O.; Austin, A. J.; Cammi, R.; Pomelli, C.; Ochterski, J. W.; Martin, R. L.; Morokuma, K.;

Zakrzewski, V. G.; Voth, G. A.; Salvador, P.; Dannenberg, J. J.; Dapprich, S.; Daniels, A. D.; Farkas, Ö.; Foresman, J. B.; Ortiz, J. V.; Cioslowski, J.; Fox, D. J. *Gaussian 09*, Revision A.02; Gaussian Inc.: Wallingford, CT, 2009.

(21) (a) Cheeseman, J. R.; Trucks, G. W.; Keith, T. A.; Frisch, M. J. *J. Chem. Phys.* **1996**, *104*, 5497. (b) Aliev, A. E.; Courtier-Murias, D.; Zhou, S. *J. Mol. Struct.: THEOCHEM* **2009**, *893*, 1. (c) Aliev, A. E.; Courtier-Murias, D. *J. Phys. Chem. B* **2007**, *111*, 14034.

(22) Ditchfield, R. *J. Chem. Phys.* **1972**, *56*, 5688.

(23) Clark, S. J.; Segall, M. D.; Pickard, C. J.; Hasnip, P. J.; Probert, M. J.; Refson, K.; Payne, M. C. *Z. Kristallogr.* **2005**, *220*, 567.

(24) Perdew, J. P.; Burke, K.; Enzernhof, M. *Phys. Rev. Lett.* **1999**, *77*, 3865.

(25) Vanderbilt, D. *Phys. Rev. B* **1990**, *41*, 7892.

(26) (a) Pickard, C. J.; Mauri, F. *Phys. Rev. B* **2001**, *63*, 245101. (b) Yates, J. R.; Pickard, C. J.; Mauri, F. *Phys. Rev. B* **2007**, *76*, 024401.

(27) Glendening, E. D.; Reed, A. E.; Carpenter, J. E.; Weinhold, F. *NBO*, Version 3.1; Chemistry Department, University of Wisconsin: Madison, WI, 1995.

(28) (a) Aliev, A. E.; Harris, K. D. M. *Magn. Reson. Chem.* **1998**, *36*, 855. (b) Aliev, A. E.; Harris, K. D. M.; Champkin, P. H. *J. Phys. Chem. B* **2005**, *109*, 23342.

(29) In the case of overlapping peaks, spectral editing techniques can be employed. See, for example, spectral editing techniques relying on differences in spin−lattice relaxation times: (a) Zumbulyadis, N. *J. Magn. Reson.* **1983**, *53*, 486. (b) Sharma, R.; Taylor, R. E.; Bouchard, L.-S. *J. Phys. Chem. C* **2011**, *115*, 3297.

(30) Müller, C.; Schajor, W.; Zimmermann, H.; Haeberlen, U. *J. Magn. Reson.* **1984**, *56*, 235.

(31) From powder X-ray diffraction, the two samples of glycine-d_5 studied in this work are assigned as monophasic samples of the α polymorph of glycine-d_5 (see Figure 1 for ^{2}H MAS NMR spectrum) and the γ polymorph of glycine-d_5 (see Figure 2 for ^{2}H MAS and CPMAS NMR spectra), with no evidence for any detectable amounts of *crystalline* impurity phases, suggesting that the impurity observed in the ^{2}H MAS NMR spectra is either noncrystalline or that the amount of the impurity phase present in the sample is lower than the detection level of the powder X-ray diffraction measurement. Taking into account the total signal intensity in the ^{2}H MAS NMR spectrum for glycine-d_5 (involving summation of the signal intensity within the spinning sidebands as well as the isotropic peaks) and the observed impurity, the integrated signal ratio of glycine to impurity is estimated to be ∼150:1 in the α polymorph (Figure 1) and ∼15:1 in the γ polymorph (Figure 2a).

(32) Edmonds, D. T.; Summers, C. P. *Chem. Phys. Lett.* **1976**, *41*, 482.

(33) (a) Despite the agreement in ^{2}H quadrupole coupling constants, the isotropic chemical shift of 7.8 ppm for the $-N^+D_3$ group reported by Müller et al.[30] is significantly different from the value (8.4 ppm) measured in the present work. However, the value estimated by Müller et al.[30] was derived from studies of the ^{2}H chemical shift tensor rather than direct measurement. To check their results, Müller et al.[30] compared the difference in isotropic chemical shifts for the two deuterons in the $>CD_2$ group, again derived from their single-crystal ^{2}H NMR studies, with that from a ^{2}H MAS NMR measurement by Alla and Lippmaa.[33b] As noted by Müller et al.:[30] "The splitting, about 0.8 ppm, compares very favorably with our number (0.9 ppm) for this quantity. The MAS result is obtained from a single spectrum. It is not subject to problems related to the combination of information from three different crystals. The good agreement of the MAS and our experiment with regard to the isotropic shift difference of the $-CD_2$ deuterons supports the reliability of the chemical-shift tensor results reported here." From the ^{2}H MAS NMR spectrum of Alla and Lippmaa[33b] recorded at a Larmor frequency of 55.3 MHz, the isotropic chemical shift for the $-N^+D_3$ group is determined to be 8.2 ppm (after subtracting the second-order shift of 0.07 ppm at 55.3 MHz from the peak maximum at 8.3 ppm), in agreement with our measurement of 8.4 ppm. (b) Alla, M.; Lippmaa, E. *Bruker Rep.* **1982**, *1*, 11.

(34) Camus, S.; Harris, K. D. M.; Johnston, R. L. *Chem. Phys. Lett.* **1997**, *276*, 186.

(35) Aliev, A. E.; Harris, K. D. M. *Struct. Bonding (Berlin, Ger.)* **2004**, *108*, 1.

(36) Gu, Z.; Ebisawa, K.; McDermott, A. *Solid State Nucl. Magn. Reson.* **1996**, *7*, 161.

(37) Taylor, R. E.; Chim, N.; Dybowski, C. *J. Mol. Struct.* **2006**, *794*, 133.

(38) Wei, Y.-C.; Wells, P. R.; Lambert, L. K. *Magn. Reson. Chem.* **1986**, *24*, 659.

(39) Stievano, L.; Tielens, F.; Lopes, I.; Folliet, N.; Gervais, C.; Costa, D.; Lambert, J.-F. *Cryst. Growth Des.* **2010**, *10*, 3657.

(40) Johnston, J. C.; Iuliucci, R. J.; Facelli, J. C.; Fitzgerald, G.; Mueller, K. T. *J. Chem. Phys.* **2009**, *131*, 144503.

(41) Margulès, L.; Demaison, J.; Boggs, J. E. *J. Mol. Struct.: THEOCHEM* **2000**, *500*, 245 and references therein.

(42) Reed, A. E.; Curtiss, L. A.; Weinhold, F. *Chem. Rev.* **1988**, *88*, 899.

(43) Regarding the influence of $n \rightarrow \sigma^*(C-H)$ delocalizations on electron densities, see (a) Reed, A. E.; Weinhold, F. *J. Chem. Phys.* **1985**, *83*, 1736. (b) Alabugin, I. V.; Manoharan, M.; Peabody, S.; Weinhold, F. *J. Am. Chem. Soc.* **2003**, *125*, 5973. (c) Chocholoušová, J.; Špirko, V.; Hobza, P. *Phys. Chem. Chem. Phys.* **2004**, *6*, 37.